Accepted to AJ

LSB Galaxies and the Tully-Fisher Relation

Aeree Chung

Department of Astronomy, Columbia University, New York, NY 10027

archung@astro.columbia.edu

J. H. van Gorkom

Department of Astronomy, Columbia University, New York, NY 10027

jvangork@astro.columbia.edu

K. O'Neil

Arecibo Observatory, HC03 Box 53995, Arecibo, PR 00612

koneil@naic.edu

and

G. D. Bothun

Department of Physics, University of Oregon, Eugene, Oregon 97403

nuts@bigmoo.uoregon.edu

ABSTRACT

We present Very Large Array (VLA) HI imaging of four low surface brightness (LSB) galaxies ([OBC97] P01-3, [OBC97] C06-1, [OBC97] C04-1, [OBC97] C04-2)[1] which were thought to strongly deviate from the Tully-Fisher (TF) relation based on Arecibo single-dish observations. We do not detect three of the four targeted LSB galaxies in HI down to a 4σ limit of 0.08Jy km s^{-1}. We find that two of the four of these LSBs have bright galaxies at projected distances of 2.6 and 2.9 arcminutes, which have contaminated the Arecibo signal. A further examination of the Arecibo sample shows that five out of the six galaxies that were found to deviate from TF have nearby bright galaxies (within 3.5 arcmin and within the observed HI velocity range), and we conclude that possibly

[1]The official (IAU) name of these objects are originated from O'Neil et al. (1997a). For convenience, however, [OBC97] will be omitted hereafter.

all but one of the non-TF galaxies are contaminated by HI from nearby galaxies. The sixth galaxy was not detected by us. A new observation by Arecibo did not confirm the earlier detection. We present the HI properties, kinematics, and rotation curves of three bright galaxies NGC 7631, KUG 2318+078, NGC 2595 which happened to be in the LSB fields and of two LSB galaxies, one of the targeted ones C04-2 and one (UGC 12535 or P01-1) that was found in the field of P01-3. The two detected LSB galaxies fall within 2σ on the TF relation. The integrated profiles of the bright galaxies are consistent with the Arecibo results both in velocity range and amplitude, which indicates that most of the extreme deviators from the TF relation must have been affected by bright companions in this earlier HI survey. A more recent determination of the sidelobe structure of the Arecibo beam supports our conclusion and shows that the degree of sidelobe contamination was much larger than could have been initially predicted. If the now unknown velocities of these non detected LSB's are within our probed velocity range then the limit to their HI mass is roughly 10^8 $M_\odot$ assuming $H_0 = 75$ km s^{-1} Mpc^{-1}. Hence, we have corrected the results found in O'Neil et al. (2000a) and have reconstructed the TF relation. These new observations then show a) a reconstructed TF relation that has relatively large scatter at all values of rotational velocity (possibly indicating the true range in disk galaxy properties) and b) the presence of at least some red, gas poor, LSB disks that indeed may be in an advanced evolutionary state as the faded remnants of their former high surface brightness actively star forming state.

Subject headings: galaxies: kinematics and dynamics — dark matter — galaxies: formation — galaxies: evolution

1. INTRODUCTION

As sensitivity has improved, many galaxies fainter than the natural sky brightness have been discovered. It has now become clear that the central disk surface brightness of spiral galaxies does not fall within a narrow range of $\mu_B(0)$=21.65±0.30 mag arcsec^{-2} as originally proposed by Freeman (1970) and that, at a given circular velocity, there is a very wide range of observed $\mu_B(0)$. As a candidate repository of abundant baryonic mass in the Universe and a significant link in the unsolved evolutionary paths of galaxies, low surface brightness galaxies (LSB, hereafter) have become a relatively new subject of study in extragalactic astronomy (Bothun et al. 1997 and references therein).

Since the distribution in surface brightness is continuous, there is no obvious definition for a low surface brightness galaxy, but, practically, many surveys define a low surface brightness system as a galaxy with a disk central surface brightness $\mu_B(0) \geq 23$ mag arcsec^{-2}, a value roughly equal to the brightness of the night sky background in the regime between 4000 and 5000 Å on a moonless night at a good astronomical observing site (Bothun 1998). Although several catalogs contained significant numbers of diffuse galaxies before the 1970s, the LSBs in those catalogs were limited to low mass galaxies and were not representative of the full range of LSB types. The discovery of LSB galaxies advanced considerably in the 1980s (Impey and Bothun 1997). To date (O'Neil et al. 1998 and references therein), three main classes of LSB galaxies have been identified: (1) dwarfs, defined by objects with scale lengths $\leq$1 kpc; (2) disk galaxies with scale lengths 1$\leq \alpha \leq$5 kpc and circular velocities in the range 80-200 km s^{-1}; and (3) giant disk galaxies with scale lengths $\geq$5 kpc.

Dwarf LSBs include both irregular (dI) and more regular spiral (dS) galaxies (Sung et al. 1998; Schombert et al. 2001). Dwarf LSB galaxies have much in common with blue compact dwarfs (BCDs): a large amount of HI, often with small OB associations, and blue colors ($B-V$ $\sim$0.5 mag). But dwarf irregulars are distinguished from BCDs by having amorphous shapes, as well as by having star-forming regions that are not centrally concentrated. Also, dwarf LSBs are known to have higher total masses (within a given surface brightness) and larger linear diameters than BCDs (Sung et al. 1998). Meanwhile, normal-size or giant LSBs are more similar to late-type spiral galaxies in their general properties, except in overall low stellar density. They have normal or rich HI contents with $M_{\rm HI}/L_B \approx 1.5$ (Schombert et al. 1990; van der Hulst et al. 1993; de Blok et al. 1996; Pickering et al. 1997) but the average HI surface densities are 6×10^{20} cm^{-2} which is below the threshold for star formation (van der Hulst et al. 1993; de Blok et al. 1996); CO emission is seldom detected in these systems (Schombert et al. 1990; O'Neil et al. 2000b). In a recent work by O'Neil et al. (2002, and references therein), only 6 out of 28 LSB galaxies observed at mm wavelength have been detected in CO. The integrated $B-V$ colors are known to be unusually blue without large, bright star-forming regions (Schombert et al. 1990; McGaugh et al. 1995; de Blok et al. 1995) but giant LSB spirals are redder than smaller LSB galaxies with a trend of redder color with increasing "diffuseness"(Sprayberry et al. 1995b).

Even though it is believed that giant LSBs may have evolutionary histories distinct from other LSBs (Matthews et al. 2001), most of the LSB galaxies are thought to be quiescent, unevolved and gas-rich systems (Schombert et al. 1990; McGaugh and Bothun 1994; McGaugh et al. 1995; de Blok et al. 1996; Matthews et al. 2001). To explain localized star formation without global star formation in the LSB galaxies, "sporadic star formation episodes and a slow evolutionary rate scenario" has been suggested (de Blok et al. 1995; Bothun et al. 1997). If the LSB galaxies evolve much slower than their high surface brightness counterparts, these systems must form less stars in a Hubble time and will thus have a higher total mass-to-light (M/L) ratio. For this reason, many groups have been studying the M/L ratio and the gas content of LSB galaxies to understand how the star formation history and evolutionary state of these systems differ from those of high surface brightness galaxies.

The luminosity-HI linewidth plane, first constructed by Tully and Fisher (1977), indirectly contains information about the variance in global M/L for disk galaxies. In simple dynamical terms, a small scatter about the TF relation can be understood if disk galaxies a) obey the virial theorem, b) have constant M/L and c) have constant $\mu_B(0)$. The mystery, of course, in the TF relation is that conditions b and c are demonstrably false. The recognition that the potentials of disk galaxies are dark matter dominated makes the existence of the TF relation very difficult to understand from first principles because, apparently, it requires that the amount of luminosity trace the dark matter in a way that scales exactly with V_c. This fine tuning requires that the baryonic mass fraction in disk galaxy potentials be nearly constant, which should be a troubling point as it implies that just enough baryonic gas creeps into these dark potentials and then has the correct star formation history to produce the right amount of light for a given V_c. In order for LSB disk galaxies to therefore comply with the TF relation requires an additional fine tuning between $\mu_B(0)$ and M/L must occur in such a way that higher M/L potentials (e.g. those with a reduced baryonic mass fraction) still produce the correct amount of light for a given V_c.

This apparent physical paradox strongly suggests that LSB galaxies which deviate from the observed TF relation must exist. Thus, searches have been conducted for any strong discrepancies from the TF relation among LSB galaxies in order to see whether or not there exists such a conspiracy, and how it could affect the star formation histories of either LSBs or normal spiral galaxies. Recently, O'Neil et al. (2000a) found six apparently extreme systems in their HI survey using Arecibo, which appear to strongly deviate from the TF relation thus opening up the manifold of disk galaxy properties. This potentially important result was highlighted by O'Neil et al. (2000a), but, unfortunately, as demonstrated in this paper, that result is an artifact of a much larger than anticpated side-lobe problem associated with the reconfiguration of the Arecibo focussing system and the subsequent change in illumination pattern on the dish.

The sample of O'Neil et al. (2000a) contains a more diverse LSB population in terms of color and size than other samples. In 1997, O'Neil, Bothun and Cornell (O'Neil et al. 1997a,b) conducted a comprehensive survey of LSB galaxies in order to obtain structural parameters such as μ_B, α, r_{25}, etc. and colors (Johnson/Cousins U, B, V, I, & R, when possible) in the Cancer and Pegasus galaxy clusters (hearafter OBC) using the University of Texas MacDonald Observatory 0.8 m telescope. In total 127 galaxies were found with $\mu_B \geqslant 22.0$ mag arcsec^{-2} including 119 newly identified LSB systems. The colors of these galaxies range continuously from very blue ($U-B$=0.56, $B-V$=0.37) to very red ($B-V$ >0.8; note that galaxies of S0a or earlier types have this $B-V$ value in general - see Figure 5 of Roberts and Haynes (1994)), which indicates that LSB galaxies at the present epoch define a wide range of evolutionary states (O'Neil et al. 1997b). Also, the OBC catalog includes many small galaxies with scale lengths less than 1 kpc. Since the redshifts were not known, the conversion from arcsec to kpc was based on an average distance either to the cluster (Pegasus or Cancer) or to the primary galaxy in the image (O'Neil et al. 1997a).

More recently, O'Neil et al. (2000a) conducted an HI survey of galaxies from the OBC catalog using the refurbished 305m Arecibo Gregorian Telescope, and detected HI emission from 43 galaxies out of the 111 LSBs in the 2000-12000 km s^{-1} range. The detected galaxies cover a similar range of properties as HSB galaxies, ranging from very blue through very red ($B-V$=-0.7 - 1.7) and from extremely gas rich through gas poor ($M_{\rm HI}/L_B$=0.1 - 50 $(M/L)_\odot$). With the determined line widths and absolute magnitudes, the authors find that only 40% of the HI detected LSB galaxies fall within

1σ of the standard high surface brightness galaxy TF relation. In addition, they find six extreme outliers (see Fig. 1). This indicates that the M/L ratios of some LSB galaxies are much higher than the values needed to compensate for low surface brightness. In order to determine the M/L more accurately and to study the detailed HI properties such as the HI distribution, the isophotal (HI) size, the local kinematics, rotation curves, and $M_{\rm HI}/M_T$, it is required to get HI synthesis images and in this paper we investigate the galaxies most discrepant from the TF relation found by O'Neil et al. (2000a). We obtained images with the VLA of four of the 43 galaxies detected in HI by O'Neil et al. (2000a) - three out of the six extreme non-TF galaxies and one galaxy which deviates from the TF relation by 2σ, using the VLA in the 3 km C-short configuration. The observations in the VLA, however, show that some of the Arecibo results are contaminated by bright galaxies, due to a significantly larger sidelobe compared to what was believed at the time of observation.

In this paper, we present the results of the VLA observations. In § 2, we summarize the observations and data reduction. In § 3, we present and discuss the HI properties of the galaxies which we have found in the field. Finally, in § 4, we compare the HI global profiles of the bright galaxies (contaminators) to the HI spectra of the LSBs obtained by O'Neil et al. (2000a) to illustrate the degree of confusion in the Arecibo HI survey caused by the extended sidelobe. In light of this, this paper then corrects the results of O'Neil et al. (2000a) and removes some of the observed TF discrepancy thus maintaining the mystery of how it is that LSB disk galaxies can populate a similar TF locus as high surface brightness galaxies.

2. OBSERVATIONS AND DATA REDUCTION

The HI imaging was done in June 2000 with the VLA in the 3 km C-short configuration. We observed three out of the six extreme departures from the TF (P01-3, C06-1, C04-1) and C04-2 which is located at the 2σ upper limit of the TF relation (see Fig. 1). The 21-cm linewidths (at the 50% level) determined by O'Neil et al. (2000a) for these sample galaxies are 375, 333, 410 and 85 km s^{-1}, with peak flux densities of 9, 8, 9 and 6 mJy (O'Neil et al. 2000a). From the known velocity widths, the bandwidth was chosen as 6.25 (for P01-3 and C06-1) and 3.125 (for C04-1 and C04-2) MHz. The data were obtained with 2 polarizations (2AC correlator mode) and 63 channels. The field of view is set by the 25 m diameter of the individual array elements. We integrated 8 hours per galaxy resulting in a 2σ column density sensitivity of 5.6 and 4.8×10^{19} cm^{-2} per channel (Δv=20.6 km s^{-1}) for P01-3 and C06-1, respectively, 2.6 and 3.2×10^{19} cm^{-2} per channel (Δv=10.3 km s^{-1}) for C04-2 and C04-2, respectively. Instrumental parameters and resulting sensitivities are listed in Table 1. [2]

Standard VLA calibration procedures were applied in AIPS. The continuum was subtracted

[2]Note that the rms per channel of P01-3 cube is worse or comparible to the cubes of C04-2 and C04-1 even though its wider channel width and this is caused by a serious solar interference on that day.

by making a linear fit to the visibility data for a range of line-free channels in both sides of the band. We chose line-free channels based on the HI spectra of O'Neil et al. (2000a). Two of the observations (P01-3 and C04-1) were seriously affected by solar interference. For these we first subtracted a model of the continuum image from the *uv* data, and then clipped *uv* data above 2 Jy for each datacube. To make the images we applied a weighting scheme intermediate between uniform and natural but closer to a natural weighting scheme to maximize sensitivity.

3. RESULT

In our VLA observations of the LSB galaxies, we detect five galaxies in total (including two LSBs: UGC 12535 (P01-1) and C04-2, from the four HI datacubes centered on the LSB galaxies. In the field of P01-3, we detect three galaxies, -NGC 7631, KUG 2318+078 and UGC 12535-but not P01-3. UGC 12535 is in fact the same as the LSB galaxy P01-1 in the OBC catalog. Likewise, in the field of C06-1, NGC 2595 was detected instead of the LSB galaxy, C06-1. In fact, the HI profiles of P01-2, P01-3 and C06-1 of O'Neil et al. (2000a) are consistent with those of KUG 2318+078, NGC 7631 and NGC 2595, respectively which implies that the HI survey of O'Neil et al. (2000a) must have been contaminated by bright neighbors. The details will be discussed in § 4. We do not see any HI from C04-1 which appears to be the only isolated LSB deviating significantly from the TF relation (Fig.1 and Fig. 2).

Below, we present the HI properties and HI maps of the galaxies which we detect from the VLA run (Jun, 2000). The extended HI properties are summarized in Table 2. The HI mass is calculated using $M_{\rm HI} = 2.36 \times 10^5 d^2 \int S_{\rm HI} dv\ M_{\odot}$, where the distance d in Mpc and the integrated HI emissivity $\int S_{\rm HI} dv$ is in Jy km s^{-1}. We assume $H_0 = 75$ km s^{-1} Mpc^{-1} in this work. The HI linewidths, W_{20} and W_{50}, were measured in three different ways: at 20% and 50% of (1) the highest peak; (2) two different peaks of each side of the systemic velocity; (3) the average of those two peaks. The differences are not larger than 10 km s^{-1} and the linewidths determined by the second method are given in the Table. The smallest HI mass that can be detected in a datacube at the position of the LSB is a 4σ signal per beam per channel. The upper limit to the HI mass is $\sim 10^8 \rm M_{\odot}$, if the LSB's are within the velocity range probed. Since we now no longer have a detection of these galaxies, we do not know their redshifts and they may lie outside the observed velocity range.

3.1. LSB galaxies

We detect HI from two LSB galaxies, UGC 12535 (Fig. 3) and C04-2 (Fig. 4).

UGC 12535 is found in the field of P01-3 and is also known as P01-1 in the OBC catalog. UGC 12535 was also in the original cluster spiral sample of Bothun et al. (1982) who failed to detect it in 21-cm and noted that it had an ususually low value of M_{HI}/L_B for its classification as a normal-sized late-type LSB galaxy with D_{25} $\approx$17.5 kpc (assuming H_0=75 km s^{-1} Mpc^{-1}). These new observations show that UGC 12535 is less than 2σ from TF relation with the corrected HI linewith, $W_{50}^{\rm Corr}$=174 km s^{-1} (see Fig. 11). Our HI mass of UGC 12535 implies an M_{HI}/L_B of 0.15 which is indeed very low. This is a relatively red LSB disk with observed color of $B-V$ = 0.82 (see both O'Neil et al. 1997a and Bothun et al. 1985) and thus represents a rare case of a LSB disk with relatively low gas content which may indeed be the faded evolutionary remains of a former HSB spiral, of which there are currently many in the Pegasus I cluster (see Bothun et al. (1982)).

Another HI detected LSB galaxy is C04-2. C04-2 is one of the newly identified LSBs in O'Neil et al. (1997a)'s CCD survey for LSB galaxies. However, in O'Neil et al. (1997a), the scale length of C04-2 is not available since they did not provide information for galaxies with King profiles or galaxies which have such irregular surface brightness profiles that they are unsuitable for a linear fit. But considering its apparent size (D$_{25}$ = 22.1$''$) and radial velocity (V_{opt} = 5168 km s^{-1}), the physical size (diameter) of C04-2 is about 7.4 kpc and it must be either of the first or second class. The HI profile of C04-2 is consistent with the HI spectrum of O'Neil et al. (2000a). Since the size of C04-2 is comparable to the beamsize itself, we could not derive the rotation. C04-2 is also one of the very red LSBs with $B-V$=1.33 and deviates from the TF by 2σ in the direction of smaller M/L.

The star formation history of LSB disk galaxies has generally been hard to understand, mostly because of the bulk of these disk galaxies are very blue but with very low current star formation rates. The simplest traditional scenario, that LSB disks are the faded remnants of HSB disks and thus represent an advanced state of disk galaxy evolution, has long been ruled out by the fact that the LSB disk is very blue and gas rich in general. This study has now produced a good candidate in UGC 12535 as a faded HSB disk. (In addition, the decontaminated red LSBs now remain as such with no known velocity. If they are indeed cluster members, as seems likely given their angular size, then they too may comprise additional examples of red LSB disks that are gas poor). On the other hand, C04-2 is very red yet has relatively high gas content which straightforwardly shows that red LSB galaxies are not necessarily gas-poor, a result consistent with O'Neil et al. (2000a). Thus, like their blue counterparts, red LSB disks are unlikely to be in the same evolutionary state at the present time.

3.2. HSB neighbors

NGC 7631 (Fig. 5) is found in the field of P01-3 with a radial velocity of 3746 km s^{-1}. We see its rotation curve declining (on both sides). The rotation velocity of 200 km s^{-1} decreases between 17 kpc and 20 kpc, beyond R$_{25}$ ($\approx$13.7 kpc), by 15$\pm$5.7 km s^{-1} ($\sim$7% of the maximum rotation velocity). Previously, Casertano and van Gorkom (1991) studied spiral galaxies which have declining rotation curves and find falling curves are more dominant in bright, compact galaxies and rising curves are more frequently found in low-luminosity galaxies. They conclude that the decrease in rotational velocity indicates a large ratio of luminous to dark mass in luminous regions of the systems, which suggests that the compactness of a galaxy is a measure of the initial spin parameter. We see a declining rotation curve from another bright, compact galaxy, KUG 2318+078 (Fig. 6), found in the field of P01-3 with 3886 km s^{-1}. KUG 2318+078 has remarkably asymmetric kinematics and the decrease of the rotational velocity is found only in one side. In the approaching side, the rotational velocity reaches at its maximum velocity, 125.0$\pm$1.8 km s^{-1} at a radius between 7 and 8 kpc, then drops by $\sim$21% to 98.6$\pm$6.0 km sec^{-1}. The HI profile is consistent with the HI spectrum of P01-2 (Fig. 8) obtained at Arecibo. KUG 2318+078 seems to be located outside of the Arecibo main beam (Fig. 9), but it must have affected P01-2 within the first sidelobe. The details will be discussed in the last section.

In the field of C06-1, NGC 2595 (Fig. 7) is found at a distance of 2.9 arcmin from C06-1 with a radial velocity of 4214 km s^{-1}. NGC 2595 has well defined spiral arms and a flat rotation curve with the maximum velocity of 325$\pm$17 km s^{-1}.

NGC 7631 and NGC 2595 fall into the middle of the standard TF, while KUG 2318+078 is located between 1σ and 2σ to the direction of over luminous for a given linewidth (Fig. 11).

4. DISCUSSION

Through VLA synthesis imaging (2000), we fail to detect HI from any of the LSB galaxies which were thought by O'Neil et al. (2000a) to deviate significantly from the TF relation. Instead, we find that the HI profiles of NGC 7631 and NGC 2595 are consistent in velocity range and amplitude with P01-3 and C06-1 observed by O'Neil et al. (2000a) using the Arecibo telescope (using the corrections found by Heiles et al. (2001)). The bright galaxies, NGC 7631 and NGC 2595 are located at 2.6 and 2.9 arcmin from P01-3 and C06-1, respectively. Therefore, we conclude that the HI profiles of P01-3 and C06-1 must have been contaminated by those bright companions. Similarly, we find that the HI profile of P01-2 of O'Neil et al. (2000a) is consistent with that of KUG 2318+078 which is 2.9 arcminute away (see Fig. 8). In none of these cases, the bright contaminators were expected to seriously affect the signal of the LSB galaxies in the center considering the beamsize of the Arecibo at 1420 MHz (3.1$\times$3.5 in Az$\times$ZA). However, recent work by Heiles et al. (2001) shows that the first sidelobe extends to $\sim$ 10 arcmin diameter and if we take this into account, the HI survey by O'Neil et al. (2000a) could have been seriously contaminated. As an attempt to save face, we point out that, at the time of the original observations (scheduled to be the first extragalactic post upgrade Arecibo observations) O'Neil et al. (2000a) would not have even undertaken these observations had they known that the post upgrade beam now contains a sidelobe which is effectively 3 times the beam size! Clearly that produced some anamolous results, which scientifically were interesting and lead to the VLA follow-up observations which then showed how severe the contamination really was.

Indeed, five out of the six LSB galaxies which were thought to deviate significantly from the

TF relation (O'Neil et al. 2000a) have bright companions within the first sidelobe of Arecibo (Fig. 10). Besides P01-3, C06-1, and P01-2, two other extreme non-TF LSB galaxies, C05-5 and C08-3, must have also been affected by the bright, nearby galaxies UGC 4416 and UGC 4308. In Table 3, we present the list of LSB galaxies and their possible contaminators with coordinates and radial velocities. Note, however, that unlike most of the LSB galaxies which have bright neighbors, P01-4 does not seem to be contaminated, even though P01-4 has a bright neighbor, NGC 7631, at a distance of 3.4 arcmin and it falls within the distance the beam to the sidelobe. It implies that the first sidelobe might be asymmetric, consistent with the results of Heiles et al. (2001). We investigated the fields of the 43 HI detected LSB galaxies in O'Neil et al. (2000a)'s sample. Excluding the five galaxies which turned out to be contaminated by bright galaxies, the rest of the HI-detected LSB galaxies are safely isolated within the first sidelobe of the Arecibo.

From this work, we conclude that we do not see any evidence of strong deviation from the TF relation for the LSB sample of (O'Neil et al. 2000a). Even though many groups have been working on this subject, there is still no agreement if there exists any fine tuning between central surface brightness and the total mass-to-light ratio that makes disk galaxies follow the TF relation. For instance, Zwaan et al. (1995) and Sprayberry et al. (1995a) find that the LSB galaxies follow the same TF relation defined by normal spiral while Persic and Salucci (1991) and Matthews et al. (1998b) find a curvature (underluminous at a given line width) at the low luminosity end of the TF for LSB galaxies.

These contradictory results may partly be due to selection effects. As Matthews et al. (1998b) point out, the star formation history and evolutionary states of LSB galaxies studied using the TF relation gives different interpretations strongly depending on the sample galaxies. For example, investigators who studied comparable to or larger than normal-sized galaxies conclude that LSB galaxies do follow the same TF relation (Zwaan et al. 1995; Sprayberry et al. 1995a), while others who included smaller LSBs find larger scatter in the TF (Matthews et al. 1998b). Here we have a good sample (OBC catalog, 1997) which is diverse in terms of sizes and colors and in fact, we see a larger scatter even if we exclude the contaminated LSBs.

In Fig. 11, we present the TF relation of O'Neil et al. (2000a)'s LSBs excluding the contaminated LSBs at B-band. Indeed B-band TF relations are often known to suffer from star formation activities or internal extinction. However, the ratio of surface brightness of the galaxy to the sky background steadily decreases as one goes to longer wavelength. Therefore, the S/N of low surface brightness systems at longer wavelength such as I-band is lower than at B-band, which still makes us rely on B-band TF relation the most rather than TF relations at any other longer wavelengths for low surface brightness galaxies (see Fig. 12). Hence, here we discuss about the TF relation of O'Neil et al. (2000a)'s LSBs only at B-band through Fig. 11.

We see a larger scatter at the low luminosity end but this is typical of most TF samples (see also McGaugh et al. (2001)). We find, M_B^{Corr}=-(6.57±0.96)logW_{50}^{Corr}-3.84±1.91 with 38 LSB galaxies which is close to the TF relation obtained by Zwaan et al. (1995) (M_B^{Corr}=-6.59logW_{50}^{Corr}-3.73±0.77

from 42 sample galaxies) but gives a larger scatter. Much of this scatter at the low luminosity end can be attributed to inclination error and/or significant non-circular motions that contributed to the observed linewidth. What is therefore more relevant is that we see significant scatter at higher linewidths (e.g. > 100 km s^{-1}) and this is almost surely reflecting the intrinsic variation in global M/L among disk galaxies of varying $\mu_B(0)$.

In this figure, LSBs are also plotted by color; very blue ($B-V$ <0.6), intermediate color (0.6$\leq B-V \leq$0.8) and very red ($B-V$ >0.8). Here we find a weak trend of scatter by colors; blue LSBs seem to have higher M/L (as Zwaan et al. (1995) or Matthews et al. (1998a) find), while no preferential direction is seen for red LSBs in their scatter. In fact, the OBC catalog contains many red small LSBs compared to previous LSB studies and from some of the red LSB samples, we find an opposite trend of the curvature which Persic and Salucci (1991) or Matthews et al. (1998b) found. However, the integrated color in this plot is drawn using $B-V$ only and it requires further study.

We learn the following from the TF of the LSB galaxies in the OBC catalog (O'Neil et al. 2000a): (1) the curvature predicted and found by Persic and Salucci (1991) & Matthews et al. (1998b) is marginally found only for the blue LSB galaxies; (2) unlike blue ($B-V < 0.4$) LSBs, very red ($B-V > 0.8$) LSB galaxies do not show any preferential direction in deviating from the standard TF; (3) a weak correlation between gas richness and the deviation from the TF, is found in agreement with the findings by Matthews et al. (1998b). This broadening of the TF relation, as found in this study, is consistent with moving away from selection effect dominated systems and towards a more representative sample of disk galaxies.

The VLA of the National Radio Astronomy Observatory is operated by Associated Universities, Inc. under a cooperative agreement with the National Science Foundation. This work has been supported in part by NSF grant AST-00-98249 to Columbia University.

REFERENCES

Bothun, G. D., Sullivan, W. T., III, and Schommer, R. A. 1982, AJ, 87, 725

Bothun, G. D., Impey, C., and McGaugh, S. 1997, PASP, 109, 745

Bothun, G. D. 1998, Scientific American, Special Issue-Magnificent Cosmos, vol. 9, Number 1, 80

Casertano, S., and van Gorkom, J. H. 1991, AJ, 101, 1231

de Blok, W. J. G., van der Hulst, J. M., and Bothun, G. D. 1995, MNRAS, 274, 235

de Blok, W. J. G., McGaugh, S. S., and van der Hulst, J. M. 1996, MNRAS, 283, 18

Freeman, K. C. 1970, ApJ, 160, 811

Heiles, C., et al. 2001, preprint (astro-ph/0107349)

Impey, C., and Bothun, G. 1997, A&A Rev., 35, 267

Matthews, L. D., van Driel, W., and Gallagher, J. S., III. 1998b, AJ, 116, 1169

Matthews, L. D., van Driel, W., and Gallagher, J. S., III. 1998a, AJ, 116, 2196

Matthews, L. D., van Driel, W., and Monnier-Ragaigne, D. 2001, A&A, 365, 1

McGaugh, S. S., and Bothun, G. D. 1994, AJ, 107, 530

McGaugh, S. S., Schombert, J. M., and Bothun, G. D. 1995, AJ, 109, 2019

McGaugh, S. S., Rubin, V. C., de Blok, W. J. G. 2001, AJ, 122, 2381

O'Neil, K., Bothun, G. D., and Cornell, M. E. 1997a, AJ, 113, 1212

O'Neil, K., Bothun, G. D., Schombert, J., Cornell, M. E., and Impey, C. D. 1997b, AJ, 114, 2448

O'Neil, K., Bothun, G. D., and Schombert, J. 1998, AJ, 116, 2776

O'Neil, K., Bothun, G. D., and Schombert, J. 2000a, AJ, 119, 136

O'Neil, K., Hofner, P., and Schinnerer, E. 2000b, ApJ, 545, L99

O'Neil et al. 2002, in preparation

Persic, M., and Salucci, P. 1991, MNRAS, 248, 325

Pickering, T. E., Impey, C. D., van Gorkom, J. H., and Bothun, G. D. 1997, AJ, 114, 1858

Roberts, M. S., and Haynes, M. P. 1994, ARA&A, 32, 115

Schombert, J., Bothun, G. D., Impey, C. D., and Mundy, L. G. 1990, AJ, 100, 1523

Schombert, J., McGaugh, S. S., and Eder, J. A. 2001, AJ, 121, 2420

Sprayberry, D., Bernstein, G. M., Impey, C. D., and Bothun, G. D. 1995a, ApJ, 438, 72

Sprayberry, D., Impey, C. D., Bothun, G. D., and Irwin, M. J. 1995b, AJ, 109, 558

Sung, E-. C. et al. 1998, ApJ, 505, 199

Tully, R. B., and Fisher, J. R. 1977, A&A, 54, 661

van der Hulst, J. M., Skillman, E. D., Smith, T. R., Bothun, G. D., McGaugh, S. S., and de Block, W. J. G. 1993, AJ, 106, 548

Zwaan, M. A., van der Hulst, J. M., de Blok, W. J. G., and McGaugh, S. S. 1995, MNRAS, 273, L35

This preprint was prepared with the AAS LaTeX macros v5.0.

Table 1. VLA observing parameters.

	P01-3	C06-1	C04-2	C04-1
Phase Center:				
R.A. (2000)[a]	23 21 18.2	08 27 31.5	08 23 29.3	08 24 33.1
Dec. (2000)[b]	08 14 29.0	21 30 04.0	21 36 45.0	21 27 04.0
Velocity Center (km s^{-1})	3746	4322	5168	7905
Velocity Range (km s^{-1})	1250	1250	630	630
Time on Source (hrs)	7.8	7.8	7.8	7.7
Bandwidth (MHz)	6.25	6.25	3.125	3.125
Number of Channels	63	63	63	63
Channel Separation (km s^{-1})	20.6	20.6	10.3	10.3
Synthesized Beam FWHM[c]	19×16	17×16	18×16	17×16
Noise level (1σ):				
-rms noise (mJy $beam^{-1}$)	0.36	0.28	0.32	0.37
-rms noise (10^{19} cm^{-2})	2.8	2.4	1.3	1.6

[a]R.A. in (h m s)

[b]Dec. in ($^\circ$ $'$ $''$)

[c]in $arcsec^2$

Table 2. General and HI properties of HI detected galaxies.

	units	LSB galaxies: UGC 12535[a]	LSB galaxies: C04-2[b]	HSB galaxies: NGC 7631[a]	HSB galaxies: KUG 2318+078[a]	HSB galaxies: NGC 2595[a]
General properties:						
Position (2000.0) -						
R.A.[c]		23 21 01.6	08 23 29.4	23 21 26.7	23 21 05.8	08 27 42.0
Dec.[d]		+08 10 45.9	+21 36 48.0	+08 13 03.0	+08 10 45.9	+21 28 44.0
Type		Sbc	Im	Sb	SBbc	Sbc
Distance	Mpc	56.2	68.9[e]	50.4	51.8	57.8
D_{25}	arcmin	1.01	0.37	1.82	1.02	2.57
i_{opt}	degrees	90.0	31.1	70.4	67.8	42.4
V_{opt}	km s^{-1}	4214	5168[c]	3778	3886	4333
$B_{\rm T}^0$	mag	14.80	17.69	13.04	14.50	12.81
HI properties:						
$S_{\rm HI}$	Jy km s^{-1}	0.62±0.18	0.13±0.08	4.5±0.20	2.6±0.18	19.9±0.17
$V_{\rm HI}$	km s^{-1}	4216±7	5168±6	3747±10	3881±5	4331±5
V_{rot}	km s^{-1}	163±15	·	180±5	55±2	325±10
$i_{\rm HI}$	degrees	23±10	·	55±2	69±4	26±2
W_{20}	km s^{-1}	202±10	107±5	383±10	162±10	331±10
W_{50}	km s^{-1}	189±10	96±5	360±10	124±10	304±10
$M_{\rm HI}$	$10^9\ M_\odot$	0.46±0.13	0.15±0.09	2.69±0.12	1.65±0.11	15.7±0.13

[a] Optical data referred to LEDA (Lyon-Meudon Extragalactic Database)

[b] Optical data referred to O'Neil et al. (1997a,b)

[c] R.A. in (h m s)

[d] Dec. in ($^\circ$ $'$ $''$)

[e] Determined by O'Neil et al. (2000a) using the Arecibo

Table 3. LSB Galaxies classified as extreme non TF and possible contaminators.

LSB Galaxies (O'Neil et al. 2000a)				Possible Contaminators[a]				Distance between two galaxies (in arcmin)
Name	R.A. (2000) h m s	Dec. (2000) $^\circ$ $'$ $''$	V_{hel} km s^{-1}	Name	R.A. (2000) h m s	Dec. (2000) $^\circ$ $'$ $''$	V_{hel} km s^{-1}	
C05-5	08 27 11.8	+22 53 47	5524	UGC 4416	08 27 16.8	+22 52 40	5533	1.67
C06-1	08 27 31.5	+21 30 04	4322	NGC 2595	08 27 42.0	+21 28 44	4330	2.94
C08-3	08 17 16.3	+21 39 14	3570	UGC 4308	08 17 25.8	+21 41 08	3566	3.04
P01-2	23 21 16.1	+08 04 54	3828	KUG 2318+078	23 21 05.8	+08 06 10	3886	2.87
P01-3	23 21 18.2	+08 14 29	3746	NGC 7631	23 21 26.7	+08 13 03	3754	2.56
P01-4	23 21 36.1	+08 15 28	3890	NGC 7631	23 21 26.7	+08 13 03	3754	3.37

[a]Data from LEDA (Lyon-Meudon Extragalactic Database)

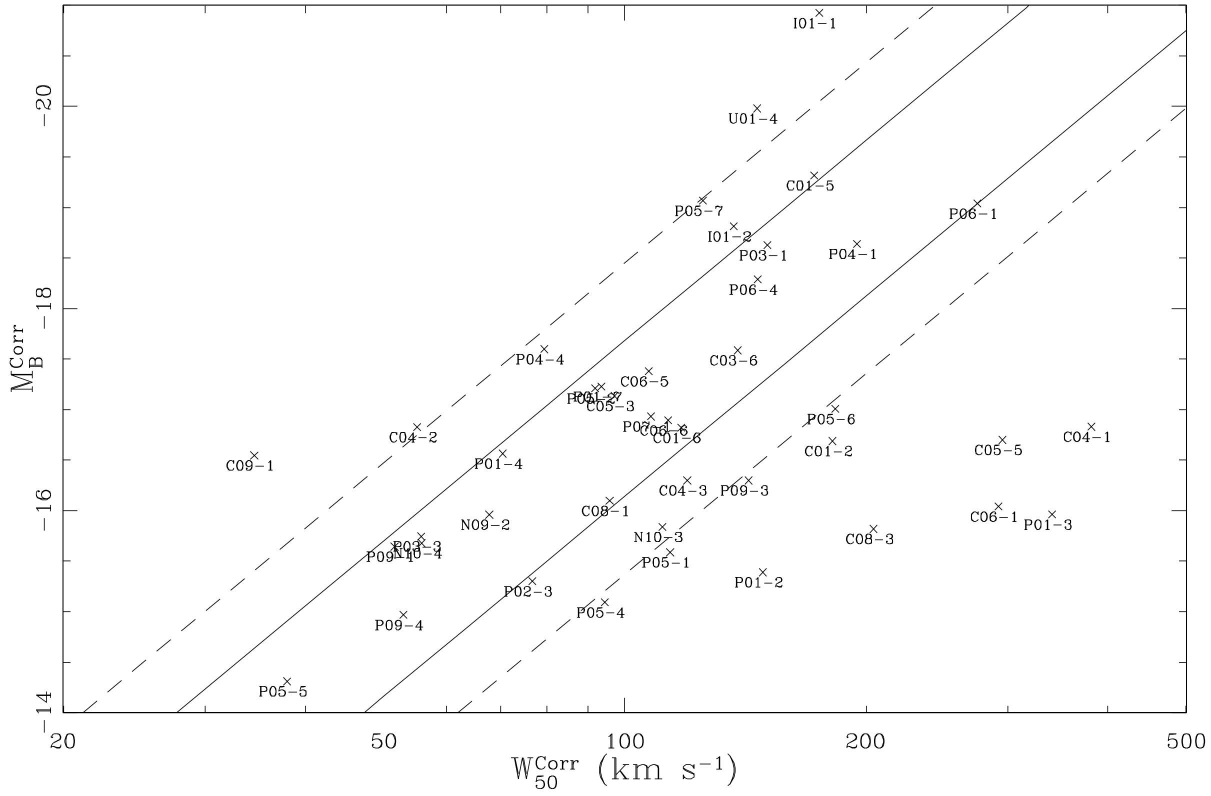

Fig. 1.— Absolute magnitudes vs. H I linewidths of LSB galaxies determined by O'Neil et al. (2000a). The absolute magnitudes were not corrected for extinction. Solid lines and dashed lines correspond to 1σ and 2σ of the LSB galaxy Tully-Fisher relation (Zwaan et al. (1995)), respectively. In this figure, we see P01-2 is quite far off from the Tully-Fisher relation instead of P09-4 which falls into the right center of the TF relation but was classified as one of the extreme non TF cases by O'Neil et al. (2000a). Note, the six most deviant points are P01-2, P01-3, C04-1, C05-5, C06-1 and C08-3.

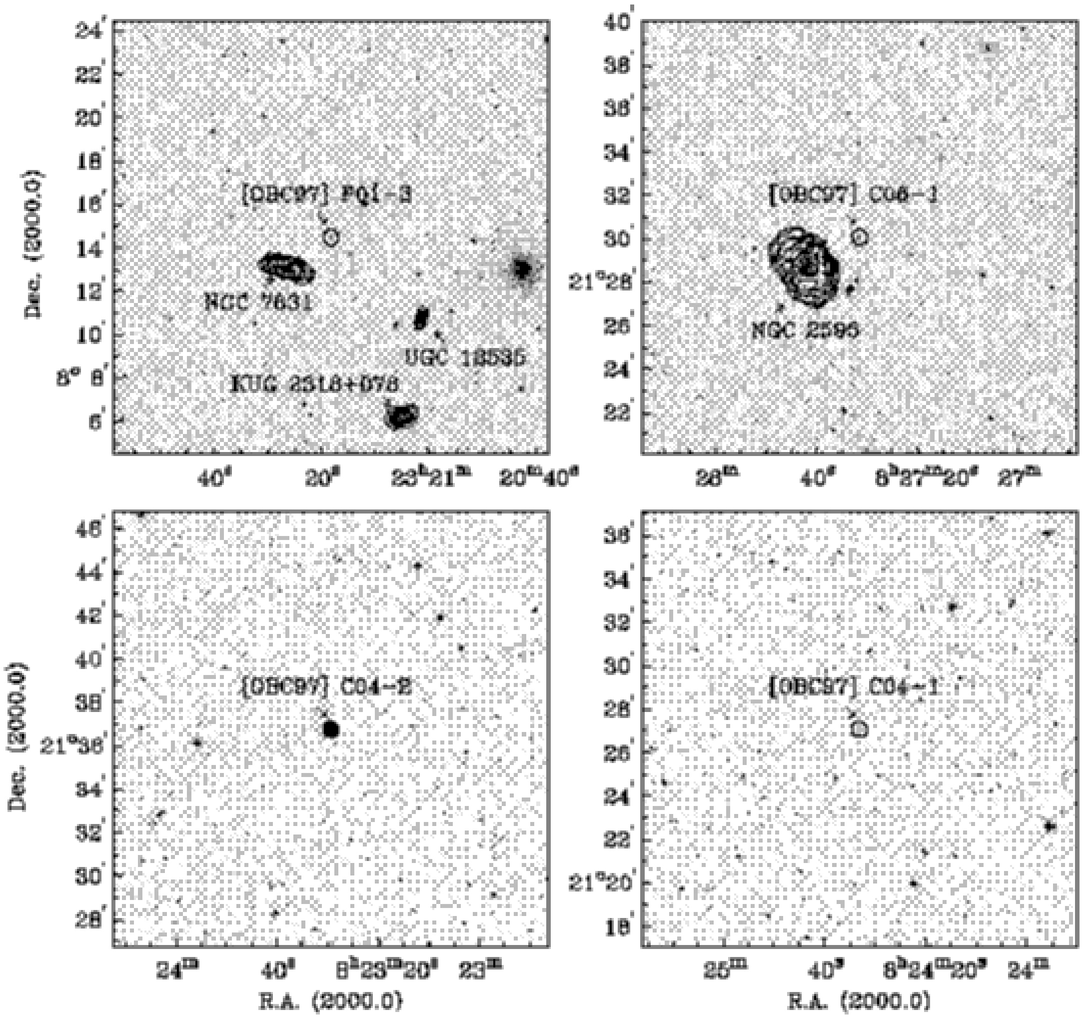

Fig. 2.— The HI contours overlaid on optical images ($20' \times 20'$). The HI images were obtained using the VLA, June, 2000. Top left) NGC 7631, KUG 2318+078, UGC12535 are found in the field of P01-3, while P01-3 does not show any HI signal. UGC 12535 is an identical object with P01-1 in OBC catalog. Top right) NGC 2595 is detected instead of C06-1. Bottom left) C04-2, one of the two HI detected LSB galaxies in the VLA run. Bottom right) We do not see any HI from C04-1 in the VLA observation even though this galaxy is apparently the only isolated extreme non TF LSB among O'Neil et al. (2000a)'s sample galaxies and a recent Arecibo observation did not confirm the previous result of O'Neil et al. (2000a).

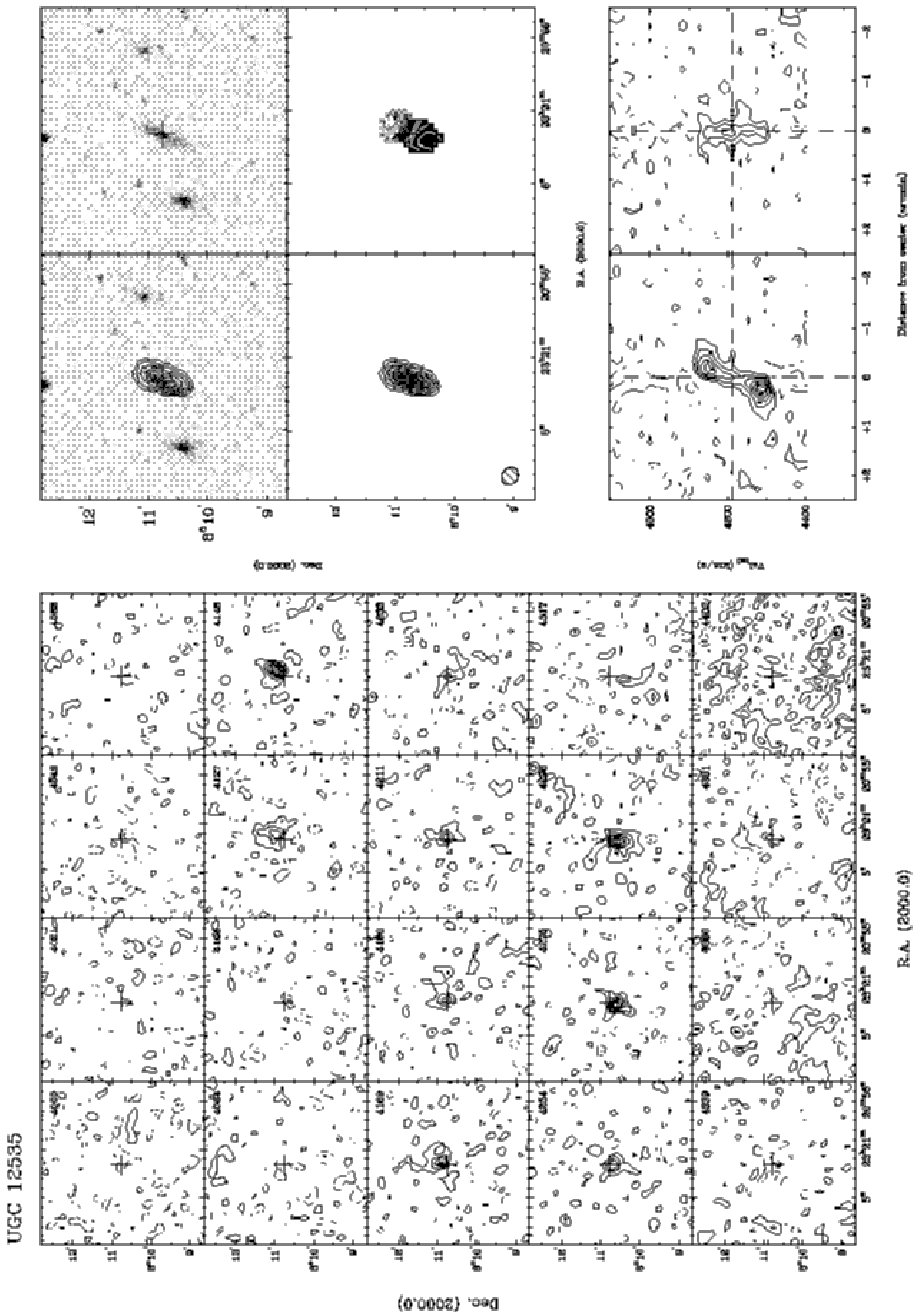

Fig. 3.— UGC 12535 ($4.25' \times 4.25'$); LSB. Left) Channel maps. The cross in each box indicates the optical center. The velocities in the upper right conners are heliocentric. Contour levels are 0.54×1, 2, 3... mJy beam^{-1} (solid lines) and -0.54×1, 2 mJy beam^{-1} (dashed lines). Right-Top) Counterclockwise from the top right, the optical image; the HI contours on the optical image (contours are $0.64+1.28\times1$, 2, 3,... 10^{19} cm^{-2} with the peak of 7.26×10^{19} cm^{-2}); the HI contours on the grayscales; the velocity field map (4216.4 ± 15 km s^{-1}). Right-Bottom) Position-velocity cuts - along the major axis (left) and the minor axis (right). Contour levels are 0.53×1, 2, 3... mJy beam^{-1} (solid lines) and -0.53×1, 2 mJy beam^{-1} (dashed lines).

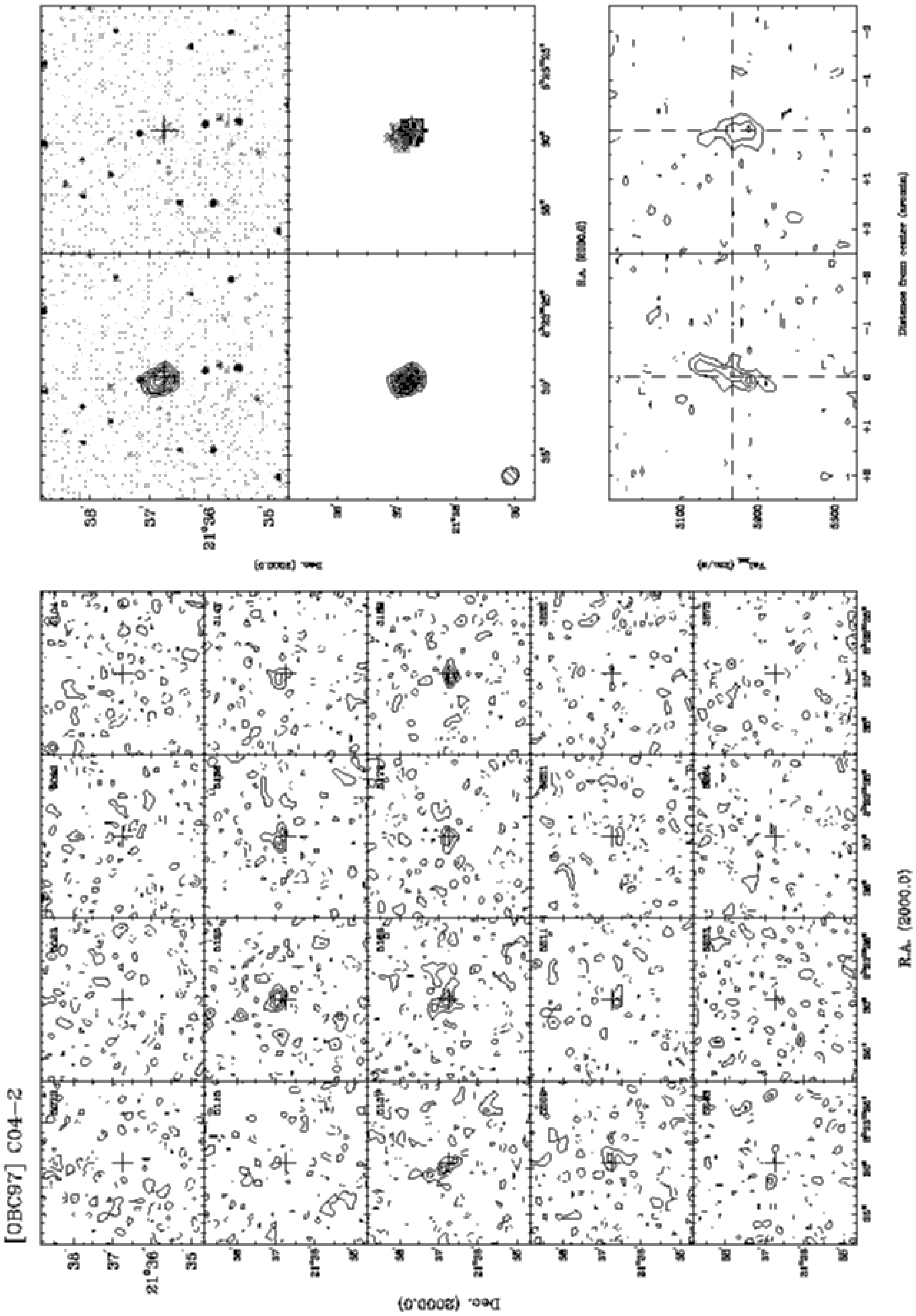

Fig. 4.— C04-2 (4.25$'$ $\times$ 4.25$'$); LSB. Left) Channel maps. The cross in each box indicates the optical center. The velocities in the upper right conners are heliocentric. Contour levels are 0.47$\times$1, 2, 3... mJy beam^{-1} (solid lines) and -0.47$\times$1, 2 mJy beam^{-1} (dashed lines). Right-Top) Counterclockwise from the top right, the optical image; the HI contours on the optical image (contours are 0.18+0.54$\times$1, 2, 3,... 10^{19} cm^{-2} with the peak of 2.59$\times10^{19}$ cm^{-2}); the HI contours on the grayscales; the velocity field map (5168$\pm$5 km s^{-1}). Right-Bottom) Position-velocity cuts - along the major axis (left) and the minor axis (right). Contour levels are 0.55$\times$1, 2, 3... mJy beam^{-1} (solid lines) and -0.55$\times$1, 2 mJy beam^{-1} (dashed lines).

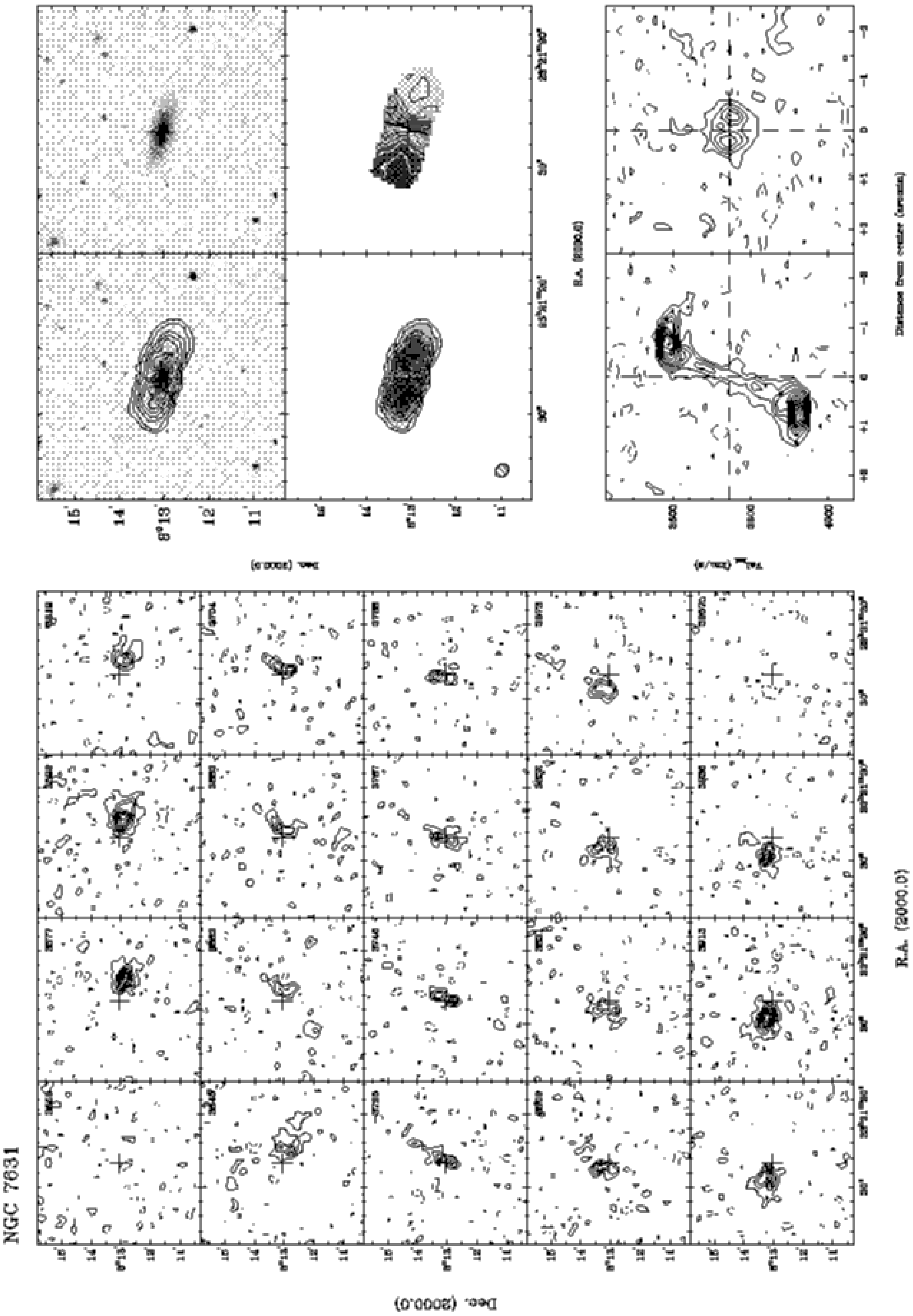

Fig. 5.— NGC 7631 (5.6′ × 5.6′). Left) Channel maps. The cross in each box indicates the optical center. The velocities in the upper right conners are heliocentric. Contour levels are 0.73×1, 2, 3... mJy beam^{-1} (solid lines) and -0.73×1, 2 mJy beam^{-1} (dashed lines). Right-Top) Counterclockwise from the top right, the optical image; the HI contours on the optical image (contours are 0.64+1.6×1, 2, 3,... 10^{19} cm^{-2} with the peak of 9.74×10^{19} cm^{-2}); the HI contours on the grayscales; the velocity field map (3771.9±25 km s^{-1}). Right-Bottom) Position-velocity cuts - along the major axis (left) and the minor axis (right). Contour levels are 0.56×1, 2, 3... mJy beam^{-1} (solid lines) and -0.56×1, 2 mJy beam^{-1} (dashed lines).

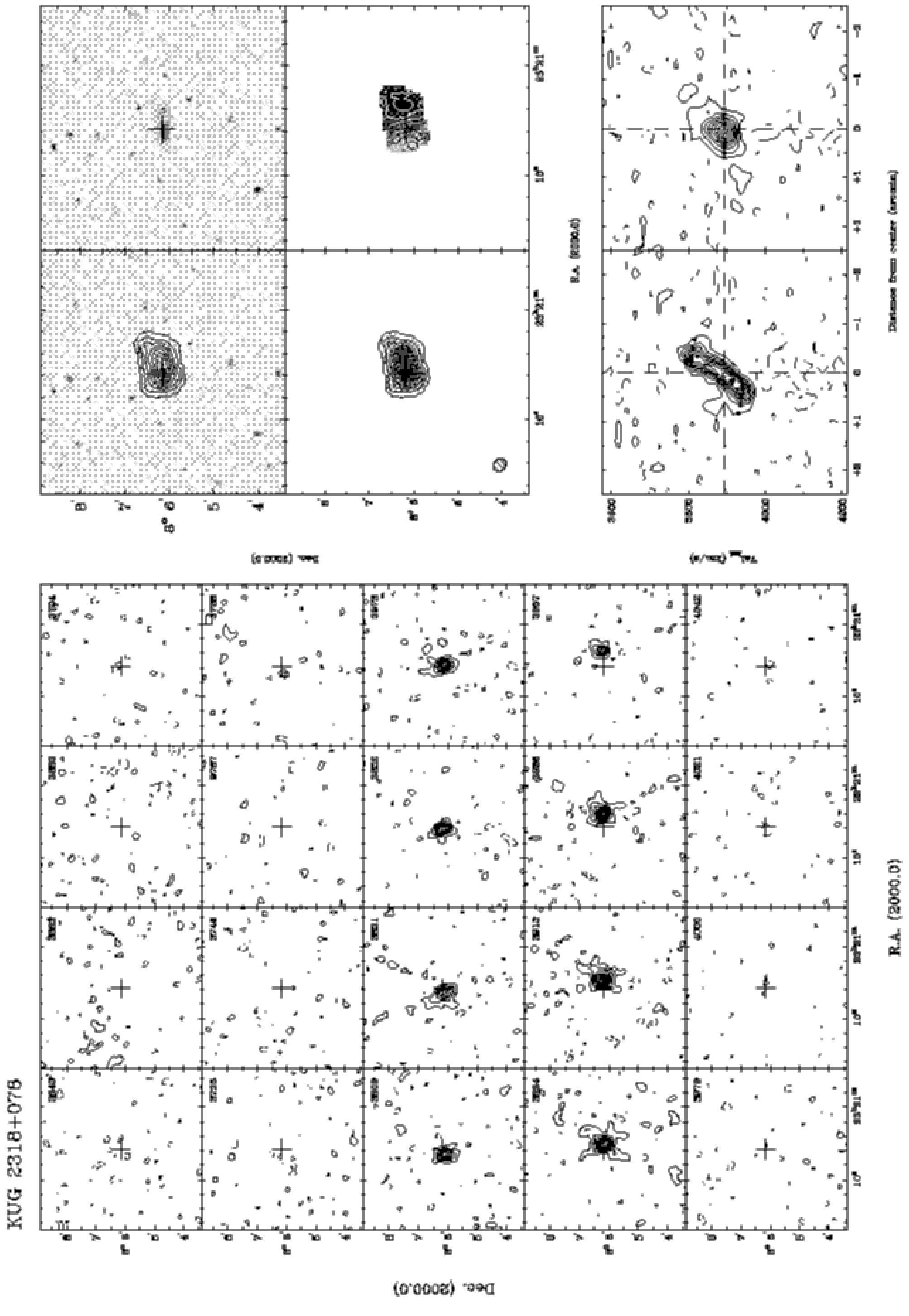

Fig. 6.— KUG 2318+078(5.6$'$ $\times$ 5.6$'$). Left) Channel maps. The cross in each box indicates the optical center. The velocities in the upper right conners are heliocentric. Contour levels are 0.78$\times$1, 2, 3... mJy beam^{-1} (solid lines) and -0.78$\times$1, 2 mJy beam^{-1} (dashed lines). Right-Top) Counterclockwise from the top right, the optical image; the HI contours on the optical image (contours are 0.64+1.92$\times$1, 2, 3,... 10^{19} cm^{-2} with the peak of 13.5$\times$$10^{19}$ cm^{-2}); the HI contours on the grayscales; the velocity field map (3896.1$\pm$15 km s^{-1}). Right-Bottom) Position-velocity cuts - along the major axis (left) and the minor axis (right). Contour levels are 0.54$\times$1, 2, 3... mJy beam^{-1} (solid lines) and -0.54$\times$1, 2 mJy beam^{-1} (dashed lines).

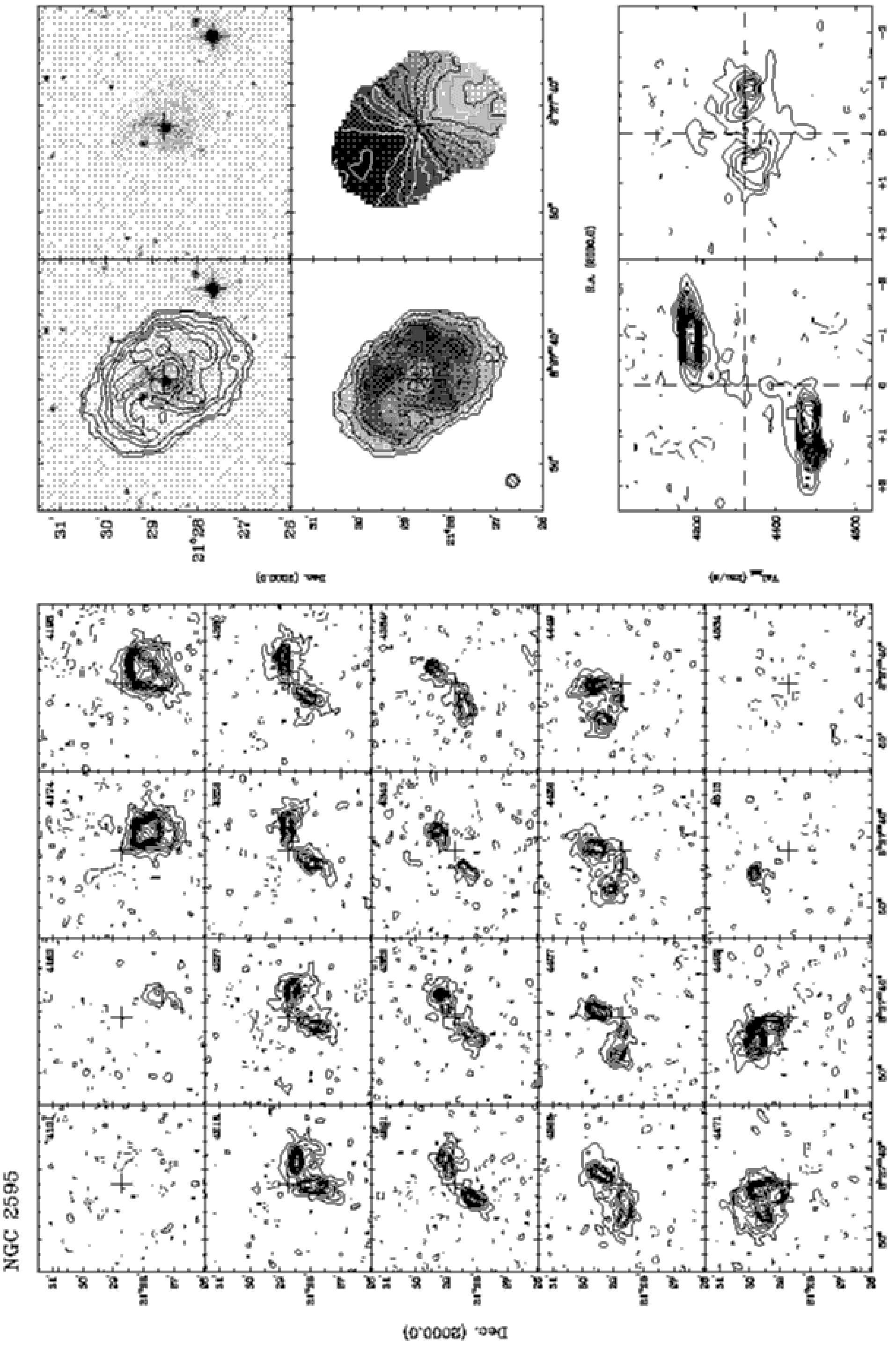

Fig. 7.— NGC 2595 (5.6$'$ × 5.6$'$). Left) Channel maps. The cross in each box indicates the optical center. The velocities in the upper right conners are heliocentric. Contour levels are 0.6×1, 2, 3... mJy beam^{-1} (solid lines) and -0.6×1, 2 mJy beam^{-1} (dashed lines). Right-Top) Counterclockwise from the top right, the optical image; the HI contours on the optical image (contours are 0.8+1.92×1, 2, 3,... 10^{19} cm^{-2} with the peak of 14.2×10^{19} cm^{-2}); the HI contours on the grayscales; the velocity field map (4330.8±25 km s^{-1}). Right-Bottom) Position-velocity cuts - along the major axis (left) and the minor axis (right). Contour levels are 0.58×1, 2, 3... mJy beam^{-1} (solid lines) and -0.58×1, 2 mJy beam^{-1} (dashed lines).

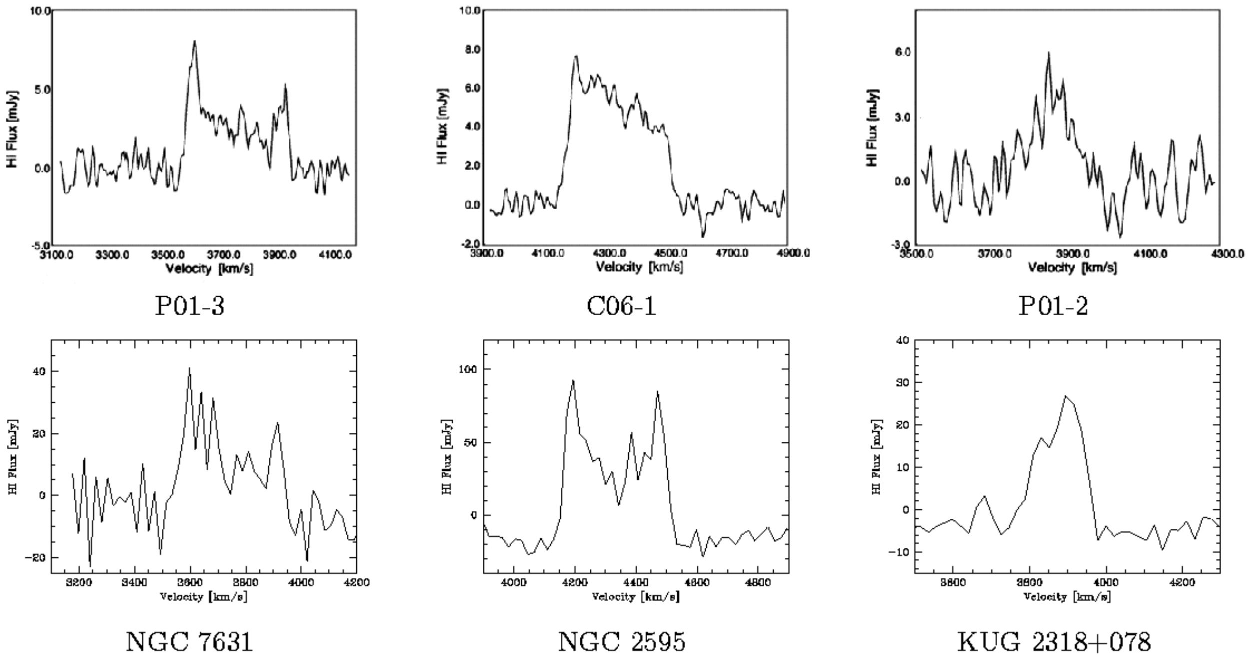

Fig. 8.— The HI profiles of the extreme non TF LSB galaxies obtained using the 305m Arecibo Gregorian Telescope (top; P01-3, C06-1, P01-2) (O'Neil et al. 2000a) and the global HI profiles of the bright systems observed with the VLA (bottom; NGC 7631, NGC 2595, KUG 2318+078). Note that the HI spectra of each pair of a LSB galaxy and its bright companion (P01-3 & NGC 7631, C06-1 & NGC 2595, P01-2 & KUG 2318+078) is consistent and the distance between the LSB system and its bright neighbor is less than 3 arcminute.

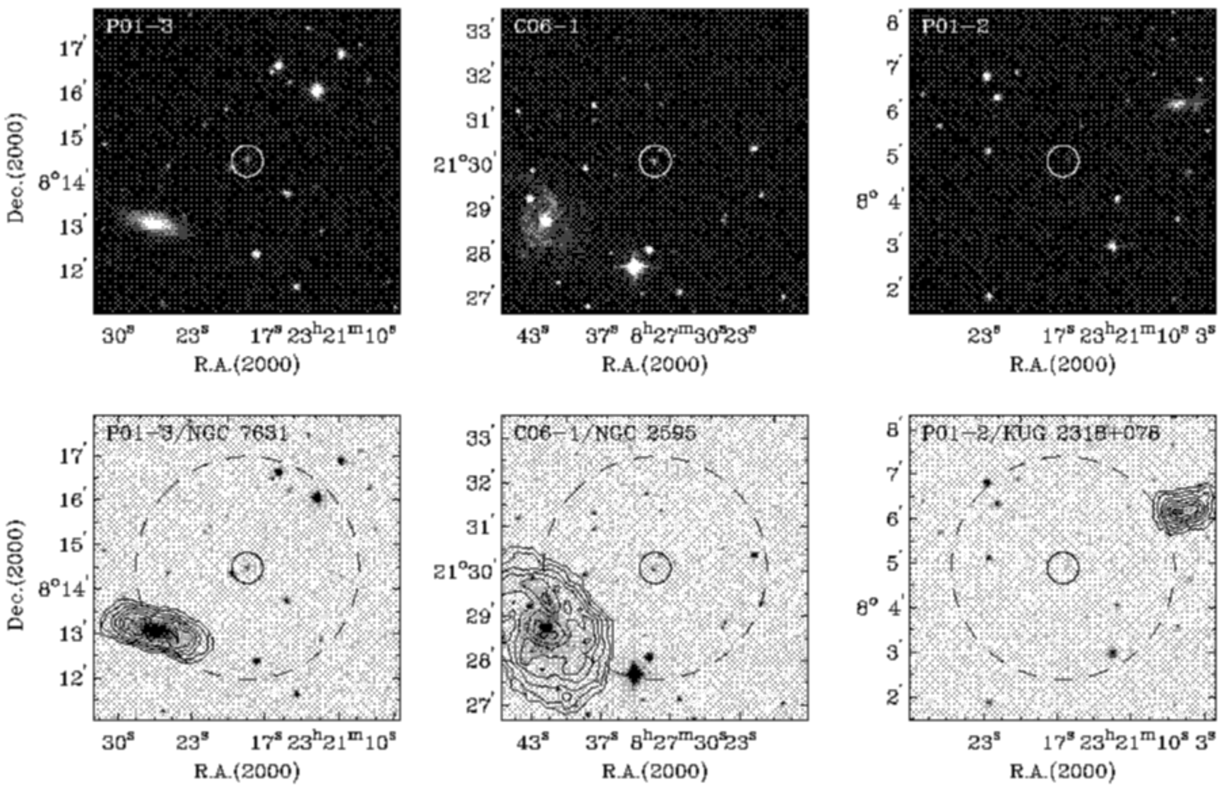

Fig. 9.— Top) Optical images of P01-3, C06-1 and P01-2 ($7^{'} \times 7^{'}$). The LSB galaxies are located inside of little circles of $0.7^{'}$ diameter. Each case has a bright companion at the close distance. Bottom) Integrated HI maps overlaid on optical images. The outer circle (the dashed line) indicates $5^{'}$ where the first sidelobe of the Arecibo reaches to the peak on the average at 1.4 GHz. Again, the inner circle is the size of $0.7^{'}$ diameter.

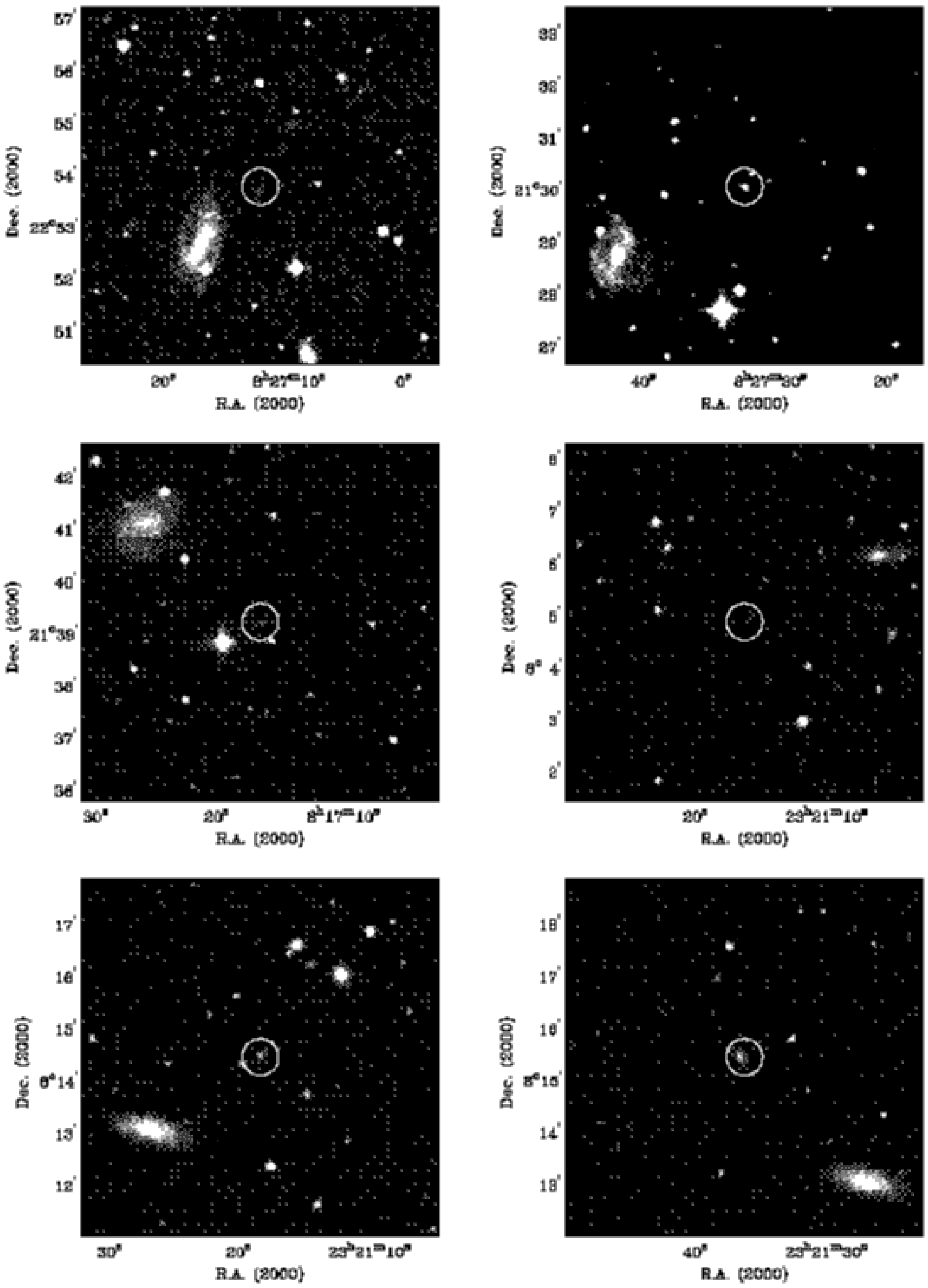

Fig. 10.— The HI detected LSB galaxies (O'Neil et al. 2000a) which have bright companions in the same velocity ranges. The LSB systems are located in the center of panels of $7^{'} \times 7^{'}$. Top (from left to right)- C05-5 & UGC 4416 and C06-1 & NGC 2595; Middle- C08-3 & UGC 4308 and P01-2 & KUG 2318+078; Bottom- P01-3 & NGC 7631 and P01-4 & NGC 7631.

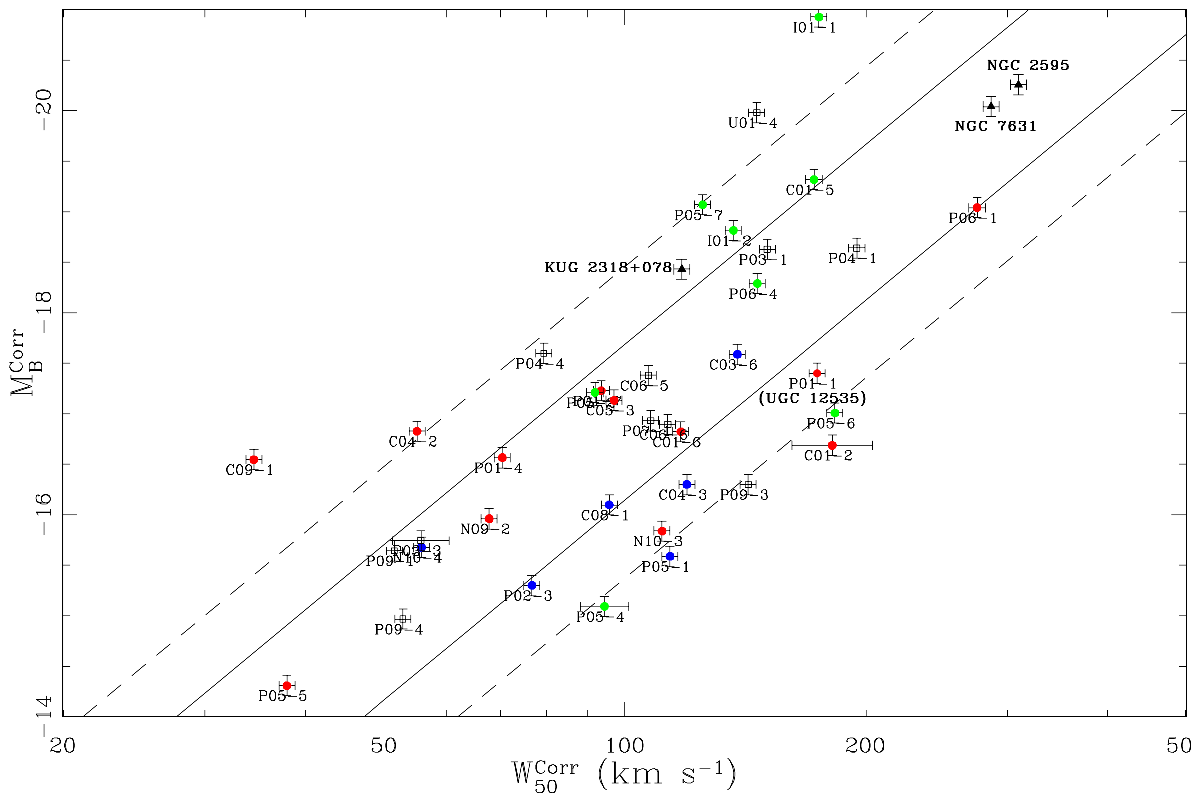

Fig. 11.— The Tully-Fisher relation for O'Neil et al. (2000a)'s sample excluding contaminated LSB galaxies. Bright galaxies, NGC 7631, NGC 2595, KUG 2318+078 (filled triangle) and one LSB galaxy P01-1 (UGC 12535) are added. Note NGC 7631 and NGC 2595 fall into the center of the TF. The empty circles indicate the very blue ($B-V$ <0.6) LSB galaxies, the filled circles indicate very red ($B-V$ >0.8) LSBs, and the stars are intermediate colors (0.6≤ $B-V$ ≤0.8). While the red LSBs (filled circles) are spread in both sides of the TF relation, the blue ones (empty circles) tend to be underluminous at a given linewidth. If LSBs are HI-detected by O'Neil et al. (2000a) but their colors are not available (O'Neil et al. 1997a), they are plotted with open squares. The errorbars indicate 1σ in both axes.

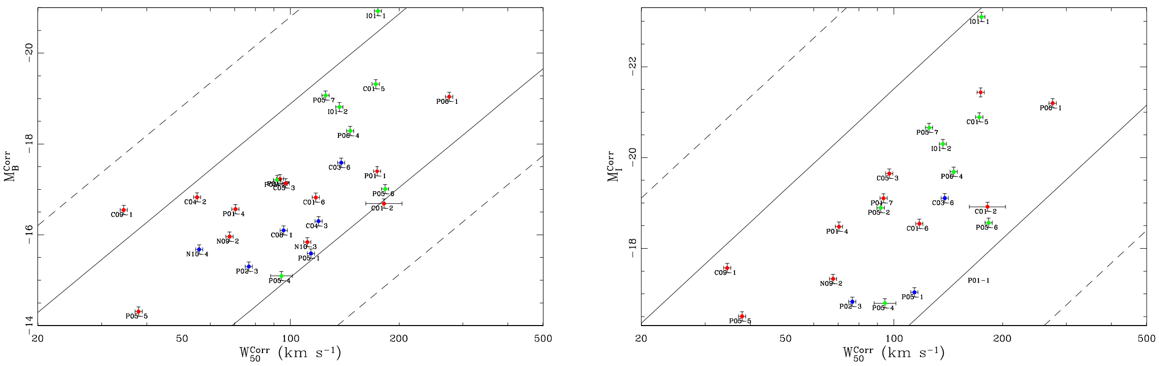

Fig. 12.— The Tully-Fisher relation: Left) in B-band; M_B^{Corr}=-6.568×log(W_{50}^{Corr})+(-3.838±1.913). The same plot as Fig. 11, but high surface brightness galaxies are dropped here. Also, instead of using the TF relation obtained by Zwaan et al. (1995), 1-σ and 2-σ lines are drawn with a newly derived TF relation with O'Neil et al. (2000a)'s sample. Right) I-band TF relation; M_I^{Corr}=-7.372×log(W_{50}^{Corr})+(-4.009±2.757). In *I*-band, it is plotted with only 21 galaxies of which magnitudes in *I*-band are available. The color classification is same as Fig. 11.